Analysis of asphalt mix surface-tread rubber interaction by using finite element method

Srirangam, Santosh Kumar; Anupam, Kumar; Kasbergen, Cor; Scarpas, Athanasios

DOI
10.1016/j.jtte.2017.07.004

Publication date
2017

Document Version
Proof

Published in
Journal of Traffic and Transportation Engineering (English Edition)

JOURNAL OF TRAFFIC AND TRANSPORTATION ENGINEERING (ENGLISH EDITION) 2017; X (X): 1–8

Available online at www.sciencedirect.com

ScienceDirect

journal homepage: www.elsevier.com/locate/jtte

Original Research Paper

Analysis of asphalt mix surface-tread rubber interaction by using finite element method

Santosh Kumar Srirangam [a], *Kumar Anupam* [b,*], *Cor Kasbergen* [b], *Athanasios (Tom) Scarpas* [b]

[a] *HSL Constructor Pte Ltd., Singapore 609162, Singapore*
[b] *Faculty of Civil Engineering and Geosciences, Delft University of Technology, Delft, The Netherlands*

HIGHLIGHTS

- Developing three-dimensional FE model to evaluate hysteretic friction.
- Revealing the micromechanical pavement surface morphology.
- Simulating different loading pressures, sliding velocities, and surfaces.
- Showing the result that hysteretic friction inversely varies with the sliding speed.

ARTICLE INFO

Article history:
Available online xxx

Keywords:
Surface texture
Hysteretic friction
Micromechanical analysis
Finite element
Contact

ABSTRACT

The surface texture of the pavement plays a very important role in driving the frictional properties at the tire rubber-pavement interface. Particularly, the hysteretic friction due to viscoelastic deformations of rubber depends mainly on the pavement surface texture. In the present paper, the effect of micromechanical pavement surface morphology on rubber block friction was brought in by comparing the friction results for three different asphalt mix morphological surfaces, named stone mastic asphalt (SMA), ultra-thin surfacing (UTS) and porous asphalt (PA). The asphalt surface morphologies of these mixes were captured by using an X-ray tomographer, from which the resulting images micromechanical finite element (FE) meshes for SMA, UTS and PA pavements were developed by means of the SimpleWare software. In the FE model, the rubber and asphalt binder were modeled as viscoelastic (VE) materials and the formulation was given in the large deformation framework. FE simulations were then carried out by using contact algorithm between rubber and the road surface. It was observed that the rubber friction inversely varies with the sliding speed and positively varies with the pressure for all the pavement morphological and stiffness conditions. Furthermore, it was observed that the highly porous pavement surface results in large dissipation of energy, hence, large rubber friction which shows that the mix characteristics of pavements have a significant effect on rubber friction.

* *Corresponding author*. Tel.: +31 15 27 82394.
E-mail addresses: santosh@hsl.com.sg (S.K. Srirangam), k.anupam@tudelft.nl (K. Anupam), c.kasbergen@tudelft.nl (C. Kasbergen), a.scarpas@tudeflt.nl (A.(T.) Scarpas).

Peer review under responsibility of Periodical Offices of Chang'an University.
http://dx.doi.org/10.1016/j.jtte.2017.07.004

1. Introduction

Tire rubber is an elastomeric material which undergoes large deformation. The contact between a rubber block and a hard, randomly rough, pavement surface is an important subject of practical application interest. Rubber friction in many cases is directly related to the internal friction of the rubber, i.e., it is a bulk property of the rubber (Grosch, 1963). When a rubber is indented onto a rough pavement surface by applying a constant pressure, the real contact area will increase with the contact time (Persson et al., 2004). In addition, if the rubber slides on a hard, rough substrate, the surface asperities of the substrate exert oscillating forces on the rubber surface leading to energy ''dissipation'' via the internal friction of the rubber (Persson and Volokitin, 2002). The force required to slide the rubber depends on the area of real contact, indentation pressure and the indentation time (Persson et al., 2004). The influence of asphalt mix characteristics on pavement surface morphology and ultimately on rubber-pavement interaction under different applied pressure and sliding speed conditions is the topic of the present research.

According to the past research studies, hysteresis was found to account for the larger part of the total friction force. Hence, in the present study, rubber friction due to the hysteresis loss is considered as the main cause of friction development. The effect of pavement macrotexture surface morphology on rubber block friction was brought in by comparing the friction results for three different asphalt mix morphological surfaces. The disparity of friction with stiffness conditions of pavement was determined by conducting the simulation analyses for non-deformable and deformable pavement surface conditions. The rubber and asphalt binder were modeled as viscoelastic (VE) materials and the formulation was given in the large deformation framework. The commercial FE package, ABAQUE/Explicit (Hibbit, Karlson & Sorensen, Inc., 2010), was used for the present analyses.

2. Description of model

In this study, the essential parameters required to simulate the interaction between tire tread block and real pavement surface morphology in macro scale are presented. The simulation of rubber-pavement surface morphology is performed under different loading pressures, sliding velocities and pavement morphological conditions described as follows.

(a) Tread rubber non-deformable pavement macrotexture interaction for SMA, UTS, and PA pavements. Such an analysis, supplements the past research studies (Klüppel and Heinrich, 1999, 2008; Persson et al., 2004) which were based on the non-deformable pavement surface conditions by simulating the rubber friction on real non-deformable asphalt pavement macrotexture conditions
(b) Tread rubber deformable pavement macrotexture interaction for UTS pavement. Such analysis emphasizes the error committed by the aforementioned analytical approaches in the determination of the friction by ignoring the deformability of the pavement surface.

2.1. Study parameters

In the present analyses, three-dimensional (3D) FE models of rubber block sliding on micromechanical pavement surface models were utilized to study the effect of pavement macrotexture morphology on rubber friction. First, 3D FE meshes of real SMA, UTS and PA pavement macrotexture morphologies were built by using X-ray tomography scans. The analysis was carried out by simulating the interaction between rubber block and pavement macrotexture under different sliding velocity and normal pressure conditions. Four sliding velocities 5, 10, 15 and 25 m/s and three pressures conditions, 200, 400 and 700 kPa were considered for this purpose. The rubber block was modeled as a viscoelastic material. In the first stage of FE simulations, the pavement surfaces were modeled as non-deformable. In the next stage of simulations, the asphalt binder was modeled as a viscoelastic (VE) material and the aggregate was modeled as a linear elastic material for all three pavements to identify the effect of pavement stiffness characteristics on rubber-pavement interaction.

2.2. Constitutive model for the viscoelastic material

In this section, the VE constitutive modelings of rubber and asphalt binder and the developments of macrotexture morphology and FE meshes for SMA, UTS, and PA are presented. Optimum dimensions of pavement surface and rubber block were selected in order to capture the effect of pavement morphology on the frictional behavior of the different material and mechanical properties. In the model, the pavement has a size of 240 mm × 40 mm × 8 mm while the rubber block has a size of 20 mm × 20 mm × 5 mm. Thermal effects have been neglected. The main assumption of the analysis is that rubber hysteretic friction is the main factor of rubber friction and the result from the internal energy dissipation of the rubber.

In the analyses, the material behaviors of the rubber and asphalt binder were characterized by means of the generalized viscoelastic model as shown in Fig. 1.

The model consists of an elastic spring in parallel with a number of Maxwell elements depending on the material representation. The Maxwell element consists of a spring and dashpot in series. The Maxwell element allows the force of the elastic spring to vary with loading rate because the viscous forces increase with the rate of deformation. In order to employ the generalized viscoelastic model, it is essential to implement viscoelastic constitutive equation into the ABAQUS numerical solving system. This can be done by calling a user-defined explicit subroutine VUMAT. ABAQUS/Explicit uses the VUMAT subroutine feature to calculate the tangent moduli of the rubber and asphalt binder.

In the model, total stress in the VE material at any time is as follow

$$\sigma = \sigma_{\infty} + \sum_{i=1}^{m} [\sigma_v]_i \quad (1)$$

Please cite this article in press as: Srirangam, S.K., et al., Analysis of asphalt mix surface-tread rubber interaction by using finite element method, Journal of Traffic and Transportation Engineering (English Edition) (2017), http://dx.doi.org/10.1016/j.jtte.2017.07.004

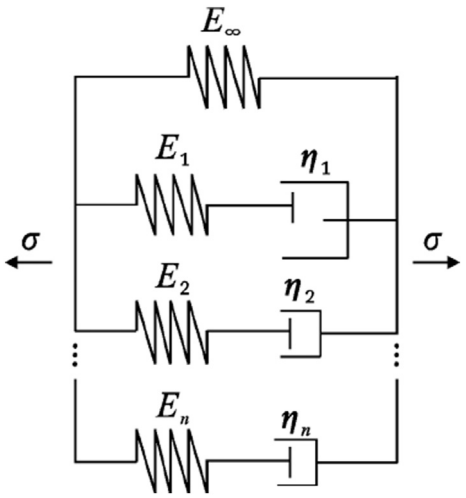

Fig. 1 – Generalized model to characterize VE properties of rubber and asphalt binder.

where σ_∞ is the stress in the equilibrium spring, σ_v is the stress in the Maxwell element, m is the number of Maxwell elements. On the basis of energy arguments and by means of multiplicative decomposition of the deformation gradient tensor (F) into elastic and viscous components.

$$F = F_e F_v \tag{2}$$

$$C_e = F_e^T F_e \tag{3}$$

$$C_v = F_v^T F_v \tag{4}$$

where F is the total deformation gradient tensor, F_v and F_e are the deformation gradient tensors associated with the viscous damper and elastic spring, respectively, C_e and C_v are the elastic and viscous right Cauchy-Green strain tensors, respectively.

The Helmholtz free energy function (ψ) is expressed as follow

$$\psi = \psi_\infty(C) + \psi_v(C_e) \tag{5}$$

where $\psi_\infty(C)$ is the equilibrium strain energy function, $\psi_v(C_e)$ is the dissipative strain energy function. The Clausius–Duhem local dissipation inequality is as follow

$$S : \frac{1}{2}\dot{C} - \dot{\psi}_v \geq 0 \tag{6}$$

$$\frac{\partial \dot{\psi}_v}{\partial \dot{C}_e}\dot{C}_e = \dot{\psi}_v \tag{7}$$

where S is the second Piola-Kirchhoff stress tensor.

It has been shown by Scarpas (2004) that the stress tensor S can be expressed as a function of viscous strain energy as follow

$$2F_v^{-1}\frac{\partial \psi_v}{\partial C_e}F_v^{-T} = S \tag{8}$$

Also, the following inequality for the dissipated energy can be obtained.

$$2C_e\frac{\partial \psi_v}{\partial C_e} : L_v \geq 0 \tag{9}$$

where $L_v = \dot{F}_v F_v^{-1}$ is the viscous velocity tensor.

The above inequality for the viscoelastic component can be further elaborated to obtain a relation between the Mandel stress Σ and L_v.

$$\Sigma : L_v \geq 0 \tag{10}$$

To satisfy the Eq. (10), the following evolution law can be postulated.

$$L_v = C_v^{-1} : \Sigma \tag{11}$$

$$C_v^{-1} = \frac{1}{2\eta_D}\left(I - \frac{1}{3}I\otimes I\right) + \frac{1}{9\eta_v}(I\otimes I) \tag{12}$$

where I is the second order identity sensor, η_D and η_v are the deviatoric and volumetric viscosities which may be dependent on the elastic left Cauchy-Green deformation sensor.

$$\eta_D = \eta_D(b_e) > 0,\ \eta_v = \eta_v(b_e) > 0,\ b_e = F_e F_e^T \tag{13}$$

2.3. Material parameters

In this study, the material data for the linear viscoelastic asphalt binder was adopted from the research study by Dai and You (2007). The binder contains sand mastic of 14% asphalt content and fine aggregates passing through a 1.18 mm sieve. The VE model for the binder comprises one equilibrium spring (E_α) and four Maxwell elements (E_i and its relaxation time, τ_i) which are connected in parallel and their parameters are shown in Table 1. The coarse aggregates of an asphalt mixture were assumed to be modeled as an elastic material with mass density of 3000 kg/m^3, Young's modulus of 55 GPa and Poisson's ratio of 0.2.

On the other hand, the material data for the linear viscoelastic rubber material in the finite strain framework was adopted from the research study by Wriggers and Nettingsmeier (2007). The rubber material was considered to be an unfilled styrene butadiene rubber (SBR) with a mass density of 1200 kg/m^3. The rubber material was assumed to be a nearly incompressible material with a Poisson's ratio of 0.49. The VE model for the rubber includes one equilibrium spring and six Maxwell elements are connected in parallel and their parameters are shown in Table 2.

2.4. FEM mesh design

The SimpleWare (ScanIP 32-bit, Version 4.3, +CAD 32-bit, Version 1.3) procedure to obtain the micromechanical FE

Table 1 – Material parameters of asphalt binder viscoelastic model (Dai and You, 2007).

Spring	VE parameter (MPa)	Dashpot	VE parameter (1/s)
E_α	59.7		
E_1	5710.6	τ_1	3.816794×10^{-2}
E_2	2075.1	τ_2	3.206150×10^{-3}
E_3	1449.0	τ_3	5.956600×10^{-4}
E_4	734.9	τ_4	5.011800×10^{-5}

Please cite this article in press as: Srirangam, S.K., et al., Analysis of asphalt mix surface-tread rubber interaction by using finite element method, Journal of Traffic and Transportation Engineering (English Edition) (2017), http://dx.doi.org/10.1016/j.jtte.2017.07.004

Table 2 – Material parameters of rubber viscoelastic model (Wriggers and Nettingsmeier, 2007).

Spring	VE parameter (MPa)	Dashpot	VE parameter (1/s)
E_α	4.2		
E_1	1.7	τ_1	1.134×10^{-2}
E_2	7.4	τ_2	2.600×10^{-4}
E_3	71.0	τ_3	1.316×10^{-5}
E_4	505.9	τ_4	1.296×10^{-6}
E_5	1125.9	τ_5	7.701×10^{-8}
E_6	1185.9	τ_6	4.200×10^{-10}

meshes for SMA, UTS and PA pavements from the images obtained from a laser profilometer and an X-ray tomographer has been explained in Section 1. The following are the salient features of the resulting FE meshes of asphalt pavement surfaces and rubber blocks that were used in the micromechanical interaction modeling.

2.5. *Asphalt pavement surface*

In this model, the SMA, UTS and PA pavements (Boscaino and Pratico, 2001; Praticò and Vaiana, 2015) were discretized by using 3D linear four-node tetrahedral (C3D4) elements for both non-deformable and deformable pavement surfaces. The non-deformable pavement meshes for SMA, UTS and PA are shown in Fig. 2(a–c). The properties of these surfaces used in the paper can be found in Tables 3–6. The non-deformability property of pavement surface can be obtained by suppressing the individual effects of asphalt binder and aggregate. In the non-deformable pavement condition, the UTS mesh consists of approximately 1 million elements, the SMA mesh consists of 0.9 million elements and the PA mesh consists of 0.8 million elements.

Table 3 – Mix compositions.

Surface	Composition (%)				
	4/10 mm	2/6.3 mm	0/4 mm	Limestone filler	Binder
PA	54.9	16.8	19.2	3.8	5.3
SMA	55.2	13.8	15.9	8.4	6.4
UTS	52.0	13.7	21.7	7.1	5.3

Unlike the rigid pavement, the flexible pavement mesh for UTS (Fig. 3) consists of both asphalt binder and aggregate elements which result in a large number of mesh elements. The total number of elements required for the flexible condition of pavement for UTS is 11.3 million. It can be understood that the computation time required would be enormous when flexible pavement conditions are employed, which necessitates the use of parallel processing computation.

2.6. *Rubber block*

In the current study, rubber block was subjected to indentation and sliding processes against the rough pavement macrotexture. Both these processes involve large deformations in the rubber block, which may lead to convergence problems, arising from a severely distorted mesh. In order to maintain a high-quality FE mesh throughout the analyses, a completely automated remeshing feature of ABAQUS/Explicit has been employed. However, because of the limitation for the automatic-meshing algorithms in ABAQUS/Explicit to produce solid brick elements, 3D linear four-node tetrahedral (C3D4) elements were used for meshing. The automated remeshing is highly computationally intensive and hence time-consuming. The current FE simulations were performed at 25 °C and the

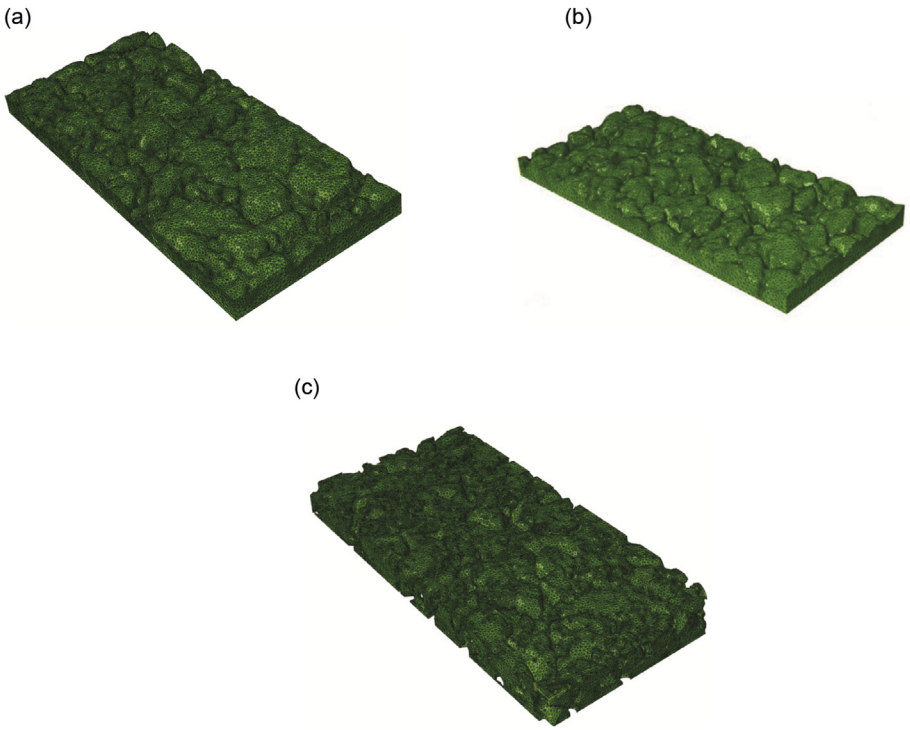

Fig. 2 – 3D view of asphalt pavement morphology. (a) SMA rigid pavement. (b) UTS rigid pavement. (c) PA rigid pavement.

Please cite this article in press as: Srirangam, S.K., et al., Analysis of asphalt mix surface-tread rubber interaction by using finite element method, Journal of Traffic and Transportation Engineering (English Edition) (2017), http://dx.doi.org/10.1016/j.jtte.2017.07.004

Table 4 – Particle size distribution of mix.

	Surface	Particle size distribution						
Passing (%)	PA	100	99	47	27	19	14	5.6
	SMA	100	90	47	29	25	21	10.1
	UTS	100	91	51	33	28	22	8.8

thermal process is considered to be isothermal in nature. The effect of temperature generation due to energy dissipation is completely neglected.

3. Modeling procedure

In general, the frictional resistance offered by the pavement roughness can be associated with the reaction forces (shear and normal) experienced by the rubber block during the sliding process. A higher contact normal force on the rubber block indicates more resistance by the pavement roughness against the action of the applied normal pressure. Hence the applied normal pressure can be related to the indentation resistance of the rubber block while the shear force can be associated to frictional resistance. The objective of this section is to identify and understand the influence of micromechanical properties of pavement surface morphology on the rubber block friction. For this purpose, the analysis is performed in two major steps: (1) indentation of the rubber block onto pavement roughness by applying normal pressure on the top surface of the block as shown in Fig. 4(a); (2) sliding the rubber block with a prescribed velocity under constant loading conditions as shown in Fig. 4(b). A frictionless contact was assumed between the bottom surface of the rubber block and pavement surface. The rubber hysteresis due to internal energy dissipation is assumed to be the main factor of friction development. To simulate the surface interaction between the rubber block and pavement surface morphology, ABAQUS/Explicit automated surface-to-surface contact algorithm was used. The resultant tangential force is computed at the top layer of the rubber block where velocity and loading conditions are applied. The ratio of the tangential force to the normal load can be defined as the sliding coefficient of friction. Various boundary conditions were tried to stimulate infinite media. Finally, the pavement geometry was considered such that its influence on the final output (skid resistance) was minimal.

4. Results

In this section, the computed friction coefficients for all the 48 cases (including 4 types of pavements, 3 applied pressures, and 4 sliding velocities) of simulation analyses of the rubber block are presented. The normal pressure and the sliding velocity conditions were varied to get a characteristic diagram of the friction coefficient.

Table 6 – Mix mean profile depth.

Surface	MPD
PA	1.146
SMA	0.461
UTS	0.632

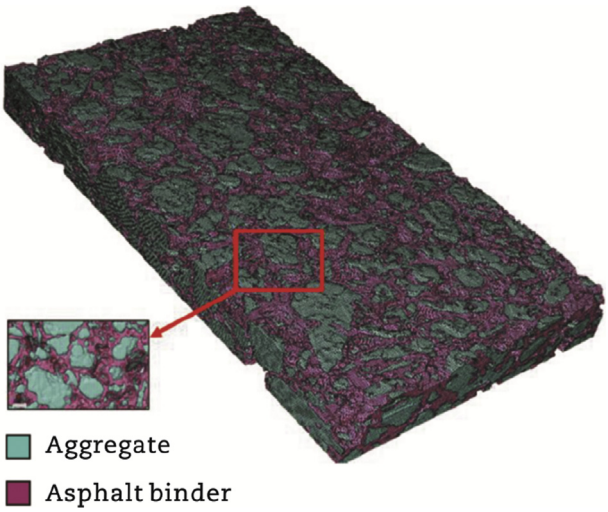

Fig. 3 – 3D view of flexible UTS pavement morphology.

4.1. *Effect of applied pressure and sliding velocity on rubber friction*

It indicates that the coefficient of sliding friction varies inversely with the sliding velocity and positively with the applied normal pressure for SMA, UTS and PA pavement macrotextures (Fig. 5). A similar trend was also observed in the flexible conditions of the UTS pavement (Fig. 6).

This type of trend is in agreement with the past research studies (Wriggers and Nettingsmeier, 2007). The rate of increase in friction coefficient was observed to be steep with increasing applied pressure and it can be taken as 0.01 to 0.05 for every sliding velocity depending on the normal pressure applied.

4.2. *Effect of asphalt mix characteristics on rubber friction*

The macrotexture corresponding to a particular asphalt surface varies greatly with its mix characteristics. If a contact occurs

Table 5 – Mix properties.

Surface	Property	Max density (kg/m^3)	Voids at 10 gyrations (%)	Voids at 50 gyrations (%)	Bulk density (kg/m^3)	Voids (%)
PA	2582	22.7	8.8	Not available	1975	23.7
SMA	2400	11.9	6.3	1.5	2294	4.4
UTS	2429	13.7	6.9	2.1	2104	13.4

Please cite this article in press as: Srirangam, S.K., et al., Analysis of asphalt mix surface-tread rubber interaction by using finite element method, Journal of Traffic and Transportation Engineering (English Edition) (2017), http://dx.doi.org/10.1016/j.jtte.2017.07.004

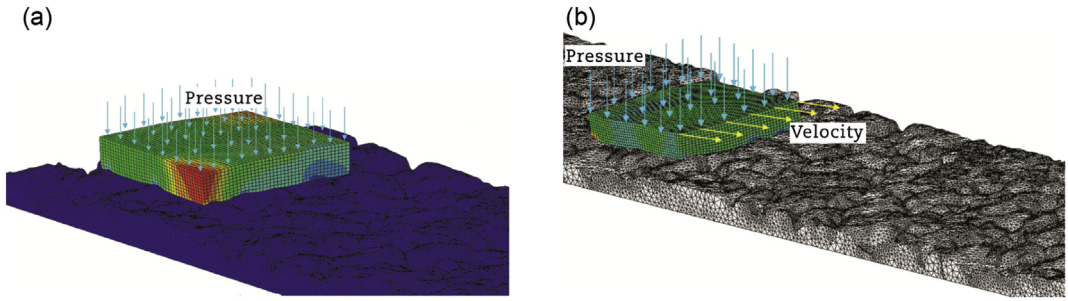

Fig. 4 – Micromechanical simulation of interaction of rubber pavement morphology. (a) Indenting the rubber block onto pavement morphology. (b) Sliding the rubber block longitudinally over the pavement morphology.

between a rubber surface and many macro-asperity contact regions of pavement surface, more hysteresis loss of the rubber takes place; hence more friction develops. In order to demonstrate this effect, an analysis was performed on SMA, UTS and PA rigid macrotexture morphological surfaces for different normal pressures and sliding velocities as shown in Fig. 7.

An examination of the results shows that the PA pavement morphology offers more frictional resistance followed by UTS surface morphology and SMA morphology. The decrease in friction coefficient from PA to UTS was observed to be 4%–26% and that from UTS to SMA was found to be 3%–13% depending on applied pressure and sliding velocity. The observed trend might be due to the asphalt mix characteristics of PA, which offers more macrotexture compared to other surface textures of the pavement.

4.3. *Effect of incorporating pavement flexibility on rubber friction*

The viscoelastic properties of asphalt binder and elastic properties for aggregate were imparted into the UTS pavement model to determine the variation of friction coefficient with respect to the stiffness of pavement surface. Fig. 8 shows the comparison of friction coefficients for rigid and flexible UTS pavement surfaces for different sliding velocity and applied pressure conditions.

This effect might be more pronounced for an actual rolling tire at higher temperature conditions of both tire rubber and asphalt binder. Under such conditions, VE properties of both rubber and asphalt binder can be greatly affected and result in the reduced energy dissipation of the tire rubber. This, in turn, results in the reduced hysteresis loss of the rubber which causes the lower skid resistance.

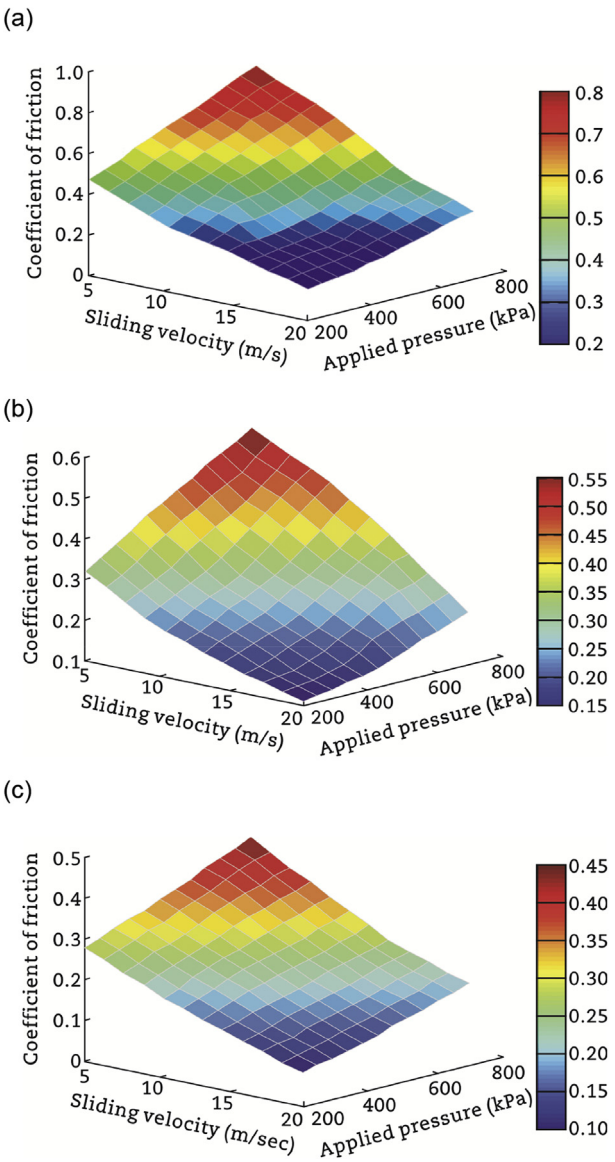

Fig. 5 – Rubber friction characterization for rigid pavement macrotexture. (a) PA pavement. (b) UTS pavement. (c) SMA pavement.

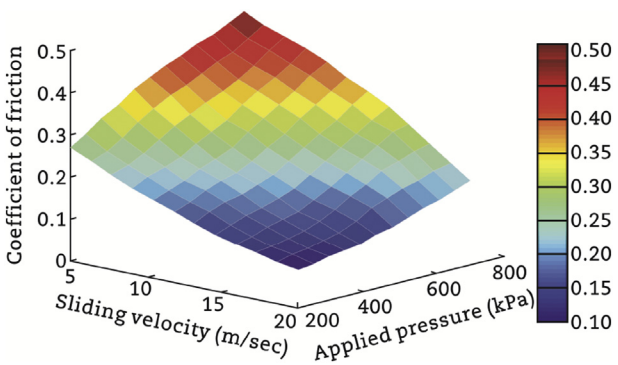

Fig. 6 – Rubber friction characterization for flexible UTS pavement macrotexture.

Please cite this article in press as: Srirangam, S.K., et al., Analysis of asphalt mix surface-tread rubber interaction by using finite element method, Journal of Traffic and Transportation Engineering (English Edition) (2017), http://dx.doi.org/10.1016/j.jtte.2017.07.004

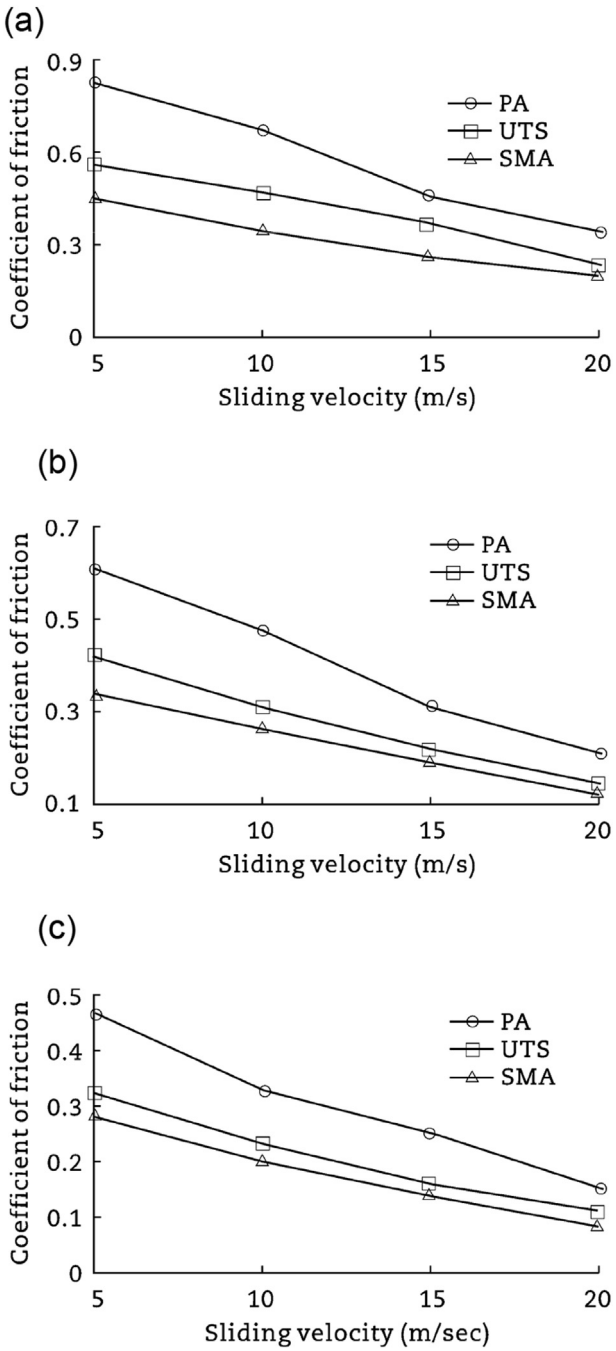

Fig. 7 – Effect of asphalt mix morphologies on rubber friction. (a) Applied pressure is 700 kPa. (b) Applied pressure is 400 kPa. (c) Applied pressure is 200 kPa.

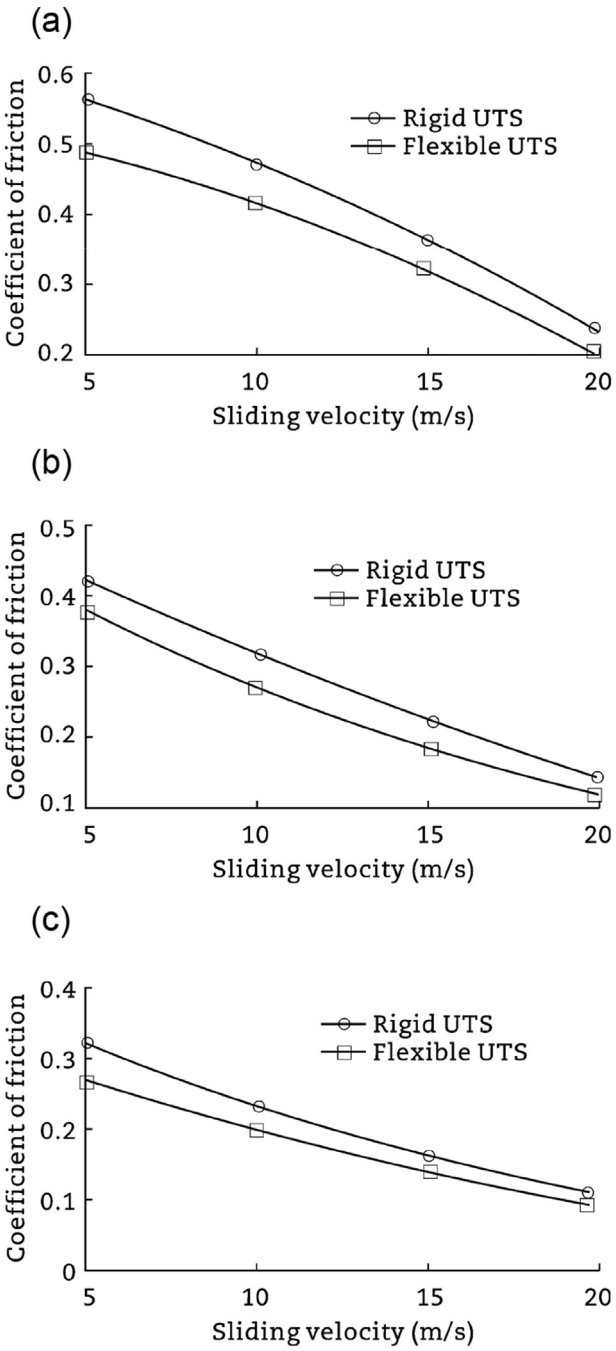

Fig. 8 – Effect of pavement flexibility on rubber friction. (a) Applied pressure is 700 kPa. (b) Applied pressure is 400 kPa. (c) Applied pressure is 200 kPa.

5. Conclusions

In the present analyses, a three-dimensional FE model was developed to find out the effect of pavement macrotexture morphology on rubber friction due to hysteresis loss. The analyses were done for different pavement stiffness, mix morphology, loading and sliding velocity conditions. It was observed that the rubber friction inversely varies with the sliding speed and positively varies with the pressure for all the pavement morphological and stiffness conditions. Furthermore, it was observed that the highly porous pavement surface results in large dissipation of energy, hence, large rubber friction which shows that the mix characteristics of pavements have a significant effect on rubber friction. It was also observed that the pavement stiffness conditions have a noticeable influence on the rubber friction coefficient; hence the individual effect of mastic and aggregate on rubber friction must be taken into account.

Please cite this article in press as: Srirangam, S.K., et al., Analysis of asphalt mix surface-tread rubber interaction by using finite element method, Journal of Traffic and Transportation Engineering (English Edition) (2017), http://dx.doi.org/10.1016/j.jtte.2017.07.004

This proposed methodology could be used to judge the performance of various mixes against skidding without the need of actual construction of a test section.

Acknowledgments

This publication was made possible by the National Priorities Research Program (NPRP) award (NPRP No. 7-482-2-184: Thermo-mechanical Tire-Pavement Interaction: Computational Modeling and Field Measurements) from the Qatar National Research Fund (a member of the Qatar Foundation). The statements made herein are solely the responsibility of the authors.

REFERENCES

Boscaino, G., Pratico, F.G., 2001. A classification of surface texture indices of pavement surfaces. Bulletin des Laboratoires des Ponts et Chaussees 234, 17–34.

Dai, Q., You, Z., 2007. Prediction of creep stiffness of asphalt mixture with micromechanical finite-element and discrete-element models. Journal of Engineering Mechanics 133 (2), 163–173.

Grosch, K.A., 1963. The relation between the friction and viscoelastic properties of rubber. Proceedings of the Royal Society A: Mathematical, Physical and Engineering Sciences 274 (1356), 21–39.

Hibbit, Karlson & Sorensen, Inc., 2010. ABAQUS 6.10, User's Manual. Hibbit, Karlson & Sorensen, Inc., Pawtucket.

Klüppel, M., Heinrich, G., 1999. Rubber friction on self-affine road tracks. Rubber Chemistry and Technology 73 (4), 578–606.

Klüppel, M., Heinrich, G., 2008. Rubber friction, tread deformation and tire traction. Wear 265 (7–8), 1052–1060.

Persson, B.N.J., Volokitin, A.I., 2002. Theory of rubber friction: nonstationary sliding. Physical Review B 65 (13), 134106.

Persson, B.N.J., Albohr, O., Creton, C., et al., 2004. Contact area between a viscoelastic solid and a hard, randomly rough, substrate. The Journal of Chemical Physics 120 (18), 8779–8793.

Praticò, F.G., Vaiana, R., 2015. A study on the relationship between mean texture depth and mean profile depth of asphalt pavements. Construction and Building Materials 101 (Part 1), 72–79.

Scarpas, A., 2004. A Mechanics Based Computational Platform for Pavement Engineering (Ph.D. thesis). Delft University of Technology, Delft.

Wriggers, P., Nettingsmeier, J., 2007. Homogenization and multiscale approaches for contact problems. Computational Contact Mechanics 498, 129–161.

Dr. Santosh Kumar Srirangam is the technical manager of HSL Constructor Pte Ltd., Singapore. He is currently involved in two prestigious national projects of Singapore, 3rd Desalination Project at Tuas and Changi Water Reclamation Project. He was a PhD scholar from Department of Civil and Structural Engineering, Delft University of Technology, The Netherlands. He authored more than 25 journal papers and conference proceedings and presented his work in various international venues. The topics of his research projects include skid resistance, constitutive modeling of materials and tire-pavement interaction. He was a member of 4 research projects during his PhD tenure at Delft University of Technology.

Dr. Kumar Anupam graduated from the Department of Civil Engineering of Indian Institute of Technology, Roorkee, India. Immediately after graduation in 2004, he worked as structural design engineer in India for two years. In the late 2006, he joined the Faculty of Civil Engineering and Environment at National University of Singapore as PhD research scholar and obtained his doctoral degree in January 2012. He is currently working as an assistant professor in the Pavement Engineering Section at TU Delft. He participated in several projects mainly related but not limited to tire-pavement interaction. He is also actively involved in organizing international courses, workshops and conferences.

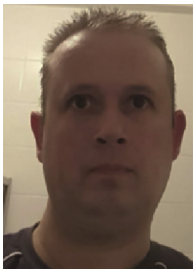

Cor Kasbergen completed his computer science MSc degree from Delft University of Technology in 1993. Directly he was employed as developer of computer aided education software by the Faculty of Civil Engineering at TU Delft. In 1997 he became permanent member of the Structural Mechanics Section of TU Delft. He has worked over the last 20 years on many mechanics related projects. Here he provided support on computational engineering issues like algorithmic stability when solving large systems of equations in pavement engineering problems. Also Kasbergen acted as the engineering coordinator in several EU projects like SKIDSAFE and Airfield Monitor

Prof. Athanasios (Tom) Scarpas is the chair and head of the Pavement Engineering Section, Delft University of Technology, The Netherlands. Prof. Scarpas research interests include constitutive modelling of pavement materials, pavement mechanics and design, chemo-mechanics of aging and healing, wheel–pavement interaction, moisture induced damage in asphalt mixtures and non-linear finite element techniques. He is an active member of numerous organizations and the Editor-in-Chief of the International Journal of Pavement Engineering. He is the recipient of an MTS professorship from the University of Minnesota and adjunct professorships from Harbin Institute of Technology and Southeast University in China.

Please cite this article in press as: Srirangam, S.K., et al., Analysis of asphalt mix surface-tread rubber interaction by using finite element method, Journal of Traffic and Transportation Engineering (English Edition) (2017), http://dx.doi.org/10.1016/j.jtte.2017.07.004